Biological Psychiatry

Archival Report

Accumulation of Lithium in the Hippocampus of Patients With Bipolar Disorder: A Lithium-7 Magnetic Resonance Imaging Study at 7 Tesla

Jacques Stout, Franz Hozer, Arthur Coste, Franck Mauconduit, Nouzha Djebrani-Oussedik, Samuel Sarrazin, Joel Poupon, Manon Meyrel, Sandro Romanzetti, Bruno Etain, Cécile Rabrait-Lerman, Josselin Houenou, Frank Bellivier, Edouard Duchesnay, and Fawzi Boumezbeur

ABSTRACT

BACKGROUND: Lithium (Li) is a first-line treatment for bipolar disorder (BD). To study its cerebral distribution and association with plasma concentrations, we used ^{7}Li magnetic resonance imaging at 7T in euthymic patients with BD treated with Li carbonate for at least 2 years.

METHODS: Three-dimensional ^{7}Li magnetic resonance imaging scans (N = 21) were acquired with an ultra-short echo-time sequence using a non-Cartesian k-space sampling scheme. Lithium concentrations ([Li]) were estimated using a phantom replacement approach accounting for differential T_1 and T_2 relaxation effects. In addition to the determination of mean regional [Li] from 7 broad anatomical areas, voxel- and parcellation-based group analyses were conducted for the first time for ^{7}Li magnetic resonance imaging.

RESULTS: Using unprecedented spatial sensitivity and specificity, we were able to confirm the heterogeneity of the brain Li distribution and its interindividual variability, as well as the strong correlation between plasma and average brain [Li] ($[Li]_B \approx 0.40 \times [Li]_P$, R = .74). Remarkably, our statistical analysis led to the identification of a well-defined and significant cluster corresponding closely to the left hippocampus for which high Li content was displayed consistently across our cohort.

CONCLUSIONS: This observation could be of interest considering 1) the major role of the hippocampus in emotion processing and regulation, 2) the consistent atrophy of the hippocampus in untreated patients with BD, and 3) the normalization effect of Li on gray matter volumes. This study paves the way for the elucidation of the relationship between Li cerebral distribution and its therapeutic response, notably in newly diagnosed patients with BD.

Keywords: Bipolar disorder (BD), Brain, High magnetic field, Hippocampus, Lithium-7 (^{7}Li), Magnetic resonance imaging (MRI)

https://doi.org/10.1016/j.biopsych.2020.02.1181

Bipolar disorder (BD) is a chronic affective disorder characterized by recurrence of manic and depressive episodes and affects 1%–3% of the adult population worldwide (1). It is a severe and debilitating illness leading to major disruptions of daily life and higher mortality, particularly by increasing the rate of suicides in affected individuals (2).

For more than half a century, lithium (Li) salts have been used to treat BD (3). Although other types of medication have appeared since, Li has remained one of the first-line drugs to treat BD (4), preventing acute manic episodes (5) and lowering the suicide rate (6). Despite decades of therapeutic use, mechanisms underlying Li effects remain largely unknown. One prevalent theory is that Li might exert neurotrophic and/or neuroprotective effects on gray matter (GM), preventing GM atrophy related to BD through inhibition of proapoptotic pathways, such as glycogen synthase kinase-3β (7). These effects seem to impact specific subcortical regions, which have been widely highlighted in the literature, particularly the hippocampus, amygdala, and thalamus (8–11). It remains unclear, however, why Li would have localized effects on specific GM volumes. One hypothesis is that the distribution of Li throughout the brain could be heterogeneous owing to a discrepancy in the density of its available transporters, especially sodium channels (12,13). There is indeed strong evidence that these channels show distinct distribution across the different regions of the human brain (14–17). The heterogeneous distribution of Li across the brain could in turn explain why its neurotrophic effects would manifest differently across

SEE COMMENTARY ON PAGE 367

the brain and across patients with BD. Indeed, only 30% of patients show an optimal outcome (18), and variability in Li response and tolerability is poorly understood.

It is at this point that nuclear magnetic resonance (NMR) provides a unique solution to detect and quantify in a noninvasive manner the local concentration of Li ([Li]). Indeed, Lithium-7 (^{7}Li), the most abundant stable Li isotope, possesses a good NMR sensitivity (~29% of ^{1}H), and its detection using in vivo ^{7}Li NMR spectroscopy has been performed successfully in animal models as well as in humans (19–21). More recently, ^{7}Li NMR spectroscopic imaging (22–25) and magnetic resonance imaging (MRI) (26–28) have been applied for the noninvasive determination of brain Li distribution in patients with BD. However, the spatial resolution and precision of those images remain limited by the low [Li] at therapeutic range (0.3–1.0 mmol/L in the plasma). Even so, those ^{7}Li-NMR studies have made important observations about Li compartmentation and its cerebral distribution (21,23,25,27,29). Yet so far, those studies have failed to identify regions of the brain where Li would accumulate significantly. We determined that such limits could be addressed by acquiring ^{7}Li MRI at 7T to improve the spatial resolution of our Li images and consequently help in determining the heterogeneity of Li distribution in the brain of euthymic patients with BD. In addition, we aimed at quantifying the total brain [Li]. For this purpose, we chose to use an ultra-short echo-time steady-state free-precession (SSFP) sequence combined with a twisted projection imaging k-space sampling scheme (30) with a reasonably short repetition time (TR) as was proposed by Boada *et al.* (31) and a quantification pipeline that we validated in a previous ex vivo preclinical study on rats pretreated with Li (29).

METHODS AND MATERIALS

Participants

Twenty-one euthymic adult outpatients with BD (10 women and 11 men, mean age ± SD = 41.2 ± 12.3 years) were recruited from the Center of Expertise for Bipolar Disorders of the Saint-Louis-Lariboisière-Fernand Widal University Hospitals (Paris, France). The criteria for inclusion were age18–65 years, a diagnosis of BD type I or type II (by DSM-IV-R criteria), scores on the Montgomery–Åsberg Depression Rating Scale (32) and Young Mania Rating Scale (33) ≤ 7, and a current daily treatment of Li carbonate extended-release tablets ingested daily for at least 2 years before inclusion. Exclusion criteria were contraindications to NMR examination and an ongoing pregnancy. Trained practitioners established the diagnosis using the Diagnostic Interview for Genetic Studies (34). Co-prescriptions (including antipsychotics, anticonvulsants, and antidepressants) and history of substance misuse were recorded. All subjects had taken their Li treatment between 8 and 10 PM in the evening before the MRI examination, which was performed systematically between 9:00 and 11:00 AM. Blood samples were drawn just before the scanning session to determine serum Li levels using inductively coupled plasma–mass spectrometry (Elan DRCe; Perkin Elmer, Courtaboeuf, France) by standard addition calibration, as previously reported (35). For each participant, response to Li was evaluated using the Retrospective Criteria of Long-Term Treatment Response in Research Subjects with Bipolar Disorder (Alda scale) (36). Clinical details are summarized in Table 1. The institutional review board and ethics committee (Comité de Protection des Personnes Ile-de-France VI) approved the study protocol in October 2016. Every patient received a complete description of the study and gave written informed consent.

Magnetic Resonance Data Acquisition

^{7}Li-NMR acquisitions were performed on a 7T Magnetom scanner (Siemens Healthineers, Erlangen, Germany) with a dual-resonance ^{1}H/^{7}Li RF birdcage coil (Rapid Biomedical, Rimpar, Germany). The protocol consisted of the acquisition of a T_1-weighted image (magnetization prepared rapid gradient echo sequence, 2-mm isotropic resolution) for anatomical reference; the acquisition of two B_0 field-maps, one for B_0 shimming and another for the correction of B_0 inhomogeneities in postprocessing; and the calibration of the reference voltage for the ^{7}Li channel using nonlocalized spectra (echo time [TE]/TR = 0.3/3000 ms), before the acquisition of the 3D ^{7}Li image (SSFP sequence, TE/TR = 0.3/200 ms, α = 20°, 1769 projections, 50% linear fraction, 352 points per spoke, 10.6-ms readout duration, 15-mm isotropic nominal resolution, 17-mm effective resolution, 24-minute acquisition time). Global T_1 and T_2 relaxation times for ^{7}Li were estimated from nonlocalized spectra acquired from a subset of our cohort of

Table 1. Demographics and Clinical Characteristics of the Cohort of Patients With Bipolar Disorder (*N* = 21)

Characteristics	Value
Categorical Variables, *n*[a]	
Male/female	11/10
Other current medication	
Antiepileptic	10
Antipsychotic	8
Antidepressant	2
Nonpsychotropic drug	4
History of substance misuse	
Tobacco	14
Alcohol	2
Cannabis	4
Others	0
Numerical Variables, Mean ± SD	
Age at MRI, years	41.2 ± 12.3
Lithium treatment duration, years	5.5 ± 3.5
Lithium dosage, mg/day	976 ± 241
Serum lithium concentration, mmol/L	0.80 ± 0.19
Erythrocyte lithium concentration, mmol/L	0.39 ± 0.19
Alda scores[b]	
Total	6.1 ± 2.5
A	7.8 ± 2.2
B	1.8 ± 1.4
MADRS	3.1 ± 2.6
YMRS	1.3 ± 1.9

MADRS, Montgomery–Åsberg Depression Rating Scale; MRI, magnetic resonance imaging; YMRS, Young Mania Rating Scale.
[a]All values represent the number of participants with the characteristic.
[b]A = Lithium response; B = weight against lithium factors; Total = A − B.

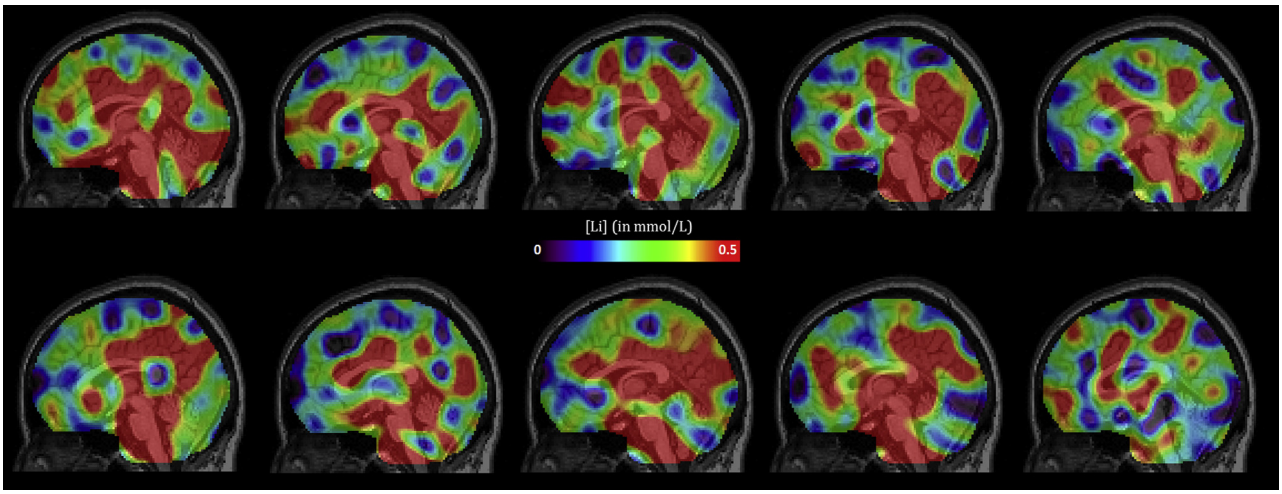

Figure 1. Gallery of lithium concentration ([Li]) maps acquired at 7T from 10 patients with bipolar disorder. Individual ^{7}Li images were interpolated at the resolution of their anatomical reference for transformation into the MNI152 template space.

patients with BD (5 out of 21) using the progressive saturation technique (37) (TR ranging from 0.4 to 20 seconds) and by varying the TE (ranging from 30 to 120 ms).

Magnetic Resonance Data Reconstruction

Non-Cartesian reconstruction of the ^{7}Li MRI was realized using a homemade Python gridding algorithm (38) with additional correction for B_0 inhomogeneities using the second experimental B_0 field-map (39–41). After [Li] maps were aligned with their ^{1}H anatomical reference, all clinical Li distribution images were interpolated and co-registered into the MNI152 space provided by the Statistical Parameter Mapping software (42).

Lithium Concentration Quantification

To estimate [Li] from the intensity of our ^{7}Li images, we adopted a modified phantom replacement approach that we validated in a previous ex vivo ^{7}Li MRI study of rats pretreated with Li (29). The same ^{7}Li MRI protocol was used to acquire at room temperature an image from a 7-L cylindrical phantom of Li chloride (50 mmol/L, pH = 7.0). Copper sulfate (1.2 g/L) was added to the solution to lower the T_1 and T_2 relaxation times of ^{7}Li in this reference phantom. In addition, in vitro T_1 and T_2 relaxation times for ^{7}Li were estimated from nonlocalized spectra acquired from this phantom using the same progressive saturation technique (37) (TR ranging from 0.4 to 20 seconds) and by varying the TE (ranging from 30 to 2000 ms). This in vitro ^{7}Li MR image was used as a 3-dimensional external reference of concentration. By considering the experimental in vivo and in vitro T_1 and T_2 relaxation times of ^{7}Li and the proper signal equation (43), individual in vivo ^{7}Li intensity images were converted into [Li] maps:

$$S_{SSFP_{FID}} \propto [Li].tan\frac{\alpha}{2}.(1-(E_1-cos\alpha).r)$$

with: $r=\sqrt{\frac{1-E_2^2}{(1-E_1cos\alpha)^2-E_2^2(E_1-cos\alpha)^2}}$ and $E_{1,2}=exp(-T_{1,2}/TR)$

Data Analysis

First, the average brain [Li] ($[Li]_B$) was estimated from the individual [Li] map (Figure 1). Then, average [Li] value were evaluated over 7 broad anatomical regions of interest (broad ROIs [bROIs]): the frontal, parietal, temporal, and occipital lobes, the brainstem, the midbrain region, and the cerebellum. These large anatomical areas are well suited for a primary description of the brain Li distribution, particularly at the individual scale. The masks were defined with a combination of probabilistic atlases provided by the FMRIB Software Library (44), in particular the Montreal Neurological Institute and Harvard-Oxford atlases (45,46). For a better visualization of the brain Li distribution across our cohort of patients, each [Li] map was normalized (i.e., the mean [Li] was set to 1.0), co-registered to the Montreal Neurological Institute brain atlas, and averaged (Figure 2). Those regional and whole-brain [Li] value were then compared with the individual plasma concentrations ($[Li]_P$) via a linear regression (Figure 3) to compute average brain-to-plasma ratios and the corresponding Pearson correlation coefficients (R) (Table 2).

As a second analysis step, we used a refined version of the Harvard-Oxford atlas covering 48 cortical and 21 subcortical areas (parcellation ROIs [pROIs]) to investigate whether Li tends to concentrate preferentially in those more specific structures. Individual [Li] maps were centered and scaled with global individual means and SDs computed over a mask of intracerebral voxels. The average of normalized images over the refined pROIs were computed and regressed onto a design matrix made of an intercept with the patient age and sex. The intercept captures the deviation of Li within each pROI from zeros, i.e., from the global individual means. Then, we computed the p values associated with the Student t test statistic corrected from multiple comparisons over the 69 pROIs using the Benjamini-Hochberg (false discovery rate) procedure (47). A standard threshold of .05 was considered on Q values (adjusted p values) for statistical significance. For visualization purpose, Figure 4 shows the statistical map at the voxel level, thresholded at $p < 10^{-3}$ and uncorrected for multiple comparisons.

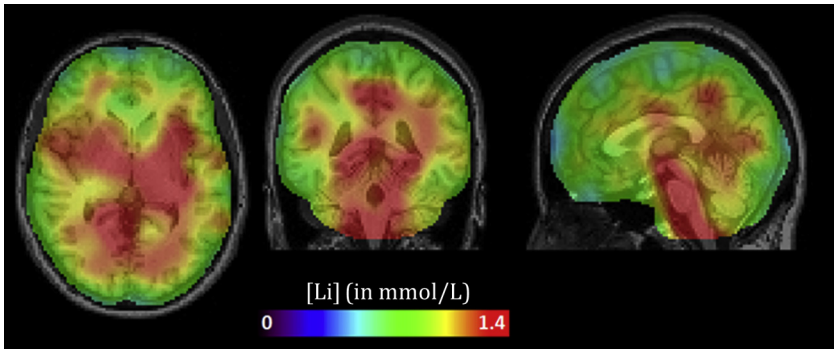

Figure 2. Normalized brain lithium distribution averaged across all our patients with bipolar disorder. Coronal, sagittal, and axial views. [Li], lithium concentration.

RESULTS

In Vivo T_1 and T_2 Relaxation Times of Lithium-7

Although ^{7}Li is a 3/2 spin with a priori biexponential longitudinal and transversal relaxation decays in complex media such as the brain (48), apparent monoexponential longitudinal and transverse relaxation times were estimated in vivo from our first 5 patients with BD at $T_{1,mono}$ = 3950 ms and $T_{2,mono}$ = 63 ms. For comparison, the T_1 and T_2 relaxation times measured for our external reference were estimated at 4.1 and 1.7 seconds, respectively.

Cerebral Lithium Distribution

As illustrated in Figure 1, the adopted ^{7}Li MRI protocol allowed us to image the whole-brain Li distribution and estimate its concentration with a satisfactory sensitivity (normalized signal-to-noise ratio of 7.3 10^{5} $mol^{-1}.min^{-½}$). As a consequence, all 21 ^{7}Li images were kept for our group analysis. For all patients, brain Li distribution was highly heterogeneous. Figure 2 shows the average normalized Li distribution across our cohort. Of note, we observed higher Li levels in the white matter and in subcortical areas. Table 2 summarizes the average (as well as the normalized) [Li] in our 7 bROIs and the whole brain. Those values confirm that higher [Li] values are observed in the brainstem, the midbrain (constituted with a large portion of white matter), and the cerebellum, while lower [Li] values could be found in the frontal and occipital lobes.

Brain-to-Plasma Lithium Comparison

As illustrated by the linear regression shown in Figure 3, we observed a good correlation between individual $[Li]_P$ and average $[Li]_B$ values. Assuming a direct proportionality, we found that $[Li]_B$ values were ~40% of $[Li]_P$ values (R = .74). As summarized in Table 2, the brain-to-plasma ratios were systematically superior to the slopes of the linear regression, ranging from 0.40 to 0.65, while the corresponding slopes ranged from 0.34 to 0.57. At the regional level, the strongest correlations were observed in the temporal and frontal lobes (R = .74 and .72, respectively), while the weakest correlations were seen in the brainstem and occipital lobes (R = .52 and .56, respectively).

Areas Where Li Is Consistently More Concentrated

Across our cohort and pROIs, [Li] was found to be significantly higher than the average $[Li]_B$ in the left hippocampus (coefficient = 1.85, SE = 0.47, 95% confidence interval [CI] = 0.87–2.83, t = 4, corrected p = .01) and in the right pallidum (coefficient = 1.98, SE = 0.58, 95% CI = 0.76–3.2, t = 3.4, corrected p = .02). At a voxel level, the statistical map thresholded at $p < 10^{-3}$ clearly fits specifically the left hippocampus shape defined in the atlas (Figure 4).

DISCUSSION

In this study, we managed to map the cerebral distribution of Li in a cohort of 21 euthymic patients with BD using ^{7}Li MRI at 7T. While $[Li]_P$ and $[Li]_B$ were strongly correlated, our results highlighted the heterogeneity of Li distribution in the brain as well as the interindividual variability of this distribution between

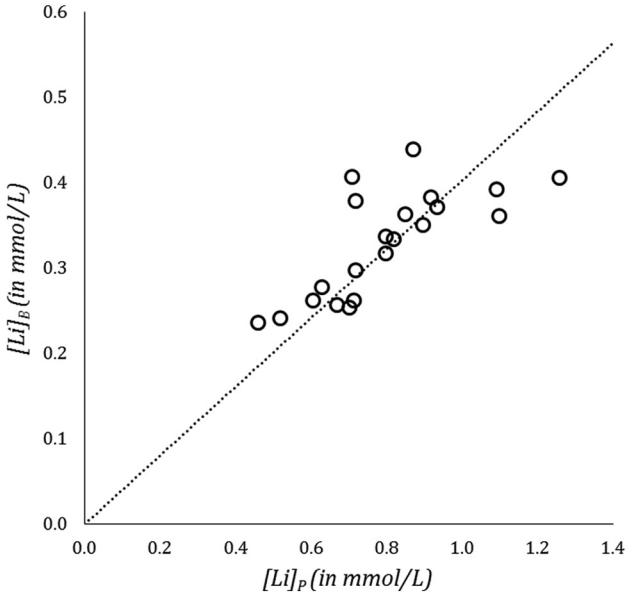

Figure 3. Average brain $[Li]_B$ vs. plasma $[Li]_P$ lithium concentrations. Overall, a good correlation between both [Li] levels was observed across our cohort, as illustrated by the linear regression, with $[Li]_B$ being ~40% of $[Li]_P$ (R = .74).

Table 2. Mean Regional Lithium Concentrations ([Li]), Normalized [Li] Levels, Brain-to-Plasma Ratios ($[Li]_B/[Li]_P$), Slopes of the Linear Regressions, and Pearson's Correlation Factors

Brain Region of Interest	[Li], mmol/L	Normalized [Li] mmol/L	$[Li]_B/[Li]_P$	Slope	*R*
Brainstem	0.46 ± 0.17	1.38 ± 0.36	0.65 ± 0.23	0.57	.52
Cerebellum	0.36 ± 0.08	1.10 ± 0.07	0.51 ± 0.12	0.44	.70
Frontal Lobe	0.28 ± 0.05	0.87 ± 0.07	0.40 ± 0.06	0.34	.72
Midbrain	0.39 ± 0.10	1.16 ± 0.11	0.54 ± 0.14	0.48	.69
Occipital Lobe	0.33 ± 0.07	1.00 ± 0.11	0.47 ± 0.10	0.40	.56
Parietal Lobe	0.32 ± 0.06	0.98 ± 0.06	0.45 ± 0.08	0.39	.71
Temporal Lobe	0.34 ± 0.08	1.03 ± 0.08	0.48 ± 0.11	0.42	.74
Whole Brain	0.33 ± 0.06	1.00	0.46 ± 0.09	0.40	.74

Values are mean ± SD, *N* = 21.

patients. Remarkably, our results suggest that the left hippocampus displayed high Li content consistently across our cohort. Finally, our data further validate the use of advanced MRI approaches to map Li—performed here in 24 minutes, a clinically feasible time.

The heterogeneity of Li distribution corroborates similar results obtained at lower spatial resolutions (24,28). It supports the hypothesis of an active transport of Li inside the brain, possibly through sodium and magnesium transporters (12,13). In particular, the distribution of sodium channels across the central nervous system is complex, owing to the molecular diversity of each subtype of sodium transporter and the differential regulation of their expression. Consequently, distinct localization patterns of those sodium channel subtypes have been observed for the different types of neurons within the brain parenchyma and the various epithelial cells at the level of the blood-brain or blood–cerebrospinal fluid barriers, leading to widely variable levels of expression and density across the brain (14–17). This could explain the heterogeneity of Li distribution in our study.

Thanks to the additional net magnetization available at 7T, we acquired our ^{7}Li images with an effective spatial resolution of 17 mm isotropic and a sensitivity threshold of ~0.05 mmol/L, thus reaching the highest spatial resolution for clinical Li imaging obtained so far. By exploiting the experimental T_1 and T_2 relaxation times of ^{7}Li in a subset of patients with BD, [Li] maps were established. Those global monoexponential $T_{1,mono}$ and $T_{2,mono}$ values were well within the range of previous reports (20,22,48). It is of interest to note here that the use of an SSFP sequence with an ultra-short TE minimizes the T_2^* weighting and reduces sensibly the T_2 weighting of the ^{7}Li image than a balanced SSFP sequence (28). Yet owing to our short TR, our quantification approach is vulnerable to local variations in T_1. Therefore, local differences in Li compartmentation (e.g., between intra- and extracellular compartments leading to varying apparent T_1 relaxation times) could contribute to the observed heterogeneity.

Our study corroborates previous studies concerning the relationship between $[Li]_P$ and $[Li]_B$ (21,24,25), with average $[Li]_B$ values ~40% of $[Li]_P$ in our study despite methodological differences. However, a stronger correlation was found in our study, probably due to the larger number of patients and the greater signal-to-noise ratio of our acquisitions.

Another favorable technical factor was the fact that our spatial resolution and our ultra-short echo-time SSFP

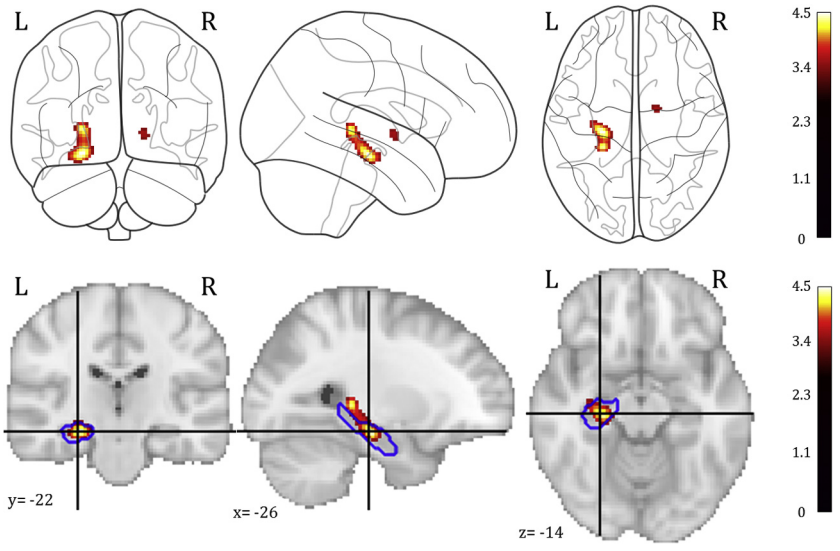

Figure 4. Voxel-based statistical map (Student's *t* test score) of increased lithium concentration over the individual mean, thresholded at $p < 10^{-3}$. Top: coronal, sagittal, and axial glass views highlight a large cluster in the left hippocampus and a small cluster in the right pallidum. Bottom: The hippocampus, as defined by the Harvard-Oxford atlas (blue contour), overlaps with our thresholded statistical map. L, left; R, right.

sequence limit the interference of Li contained in the cerebrospinal fluid compared with other in vivo ^{7}Li MRI studies (28). Still, this interference can be felt through the larger variabilities and lesser correlations observed for ROIs close to the ventricles (such as the midbrain or the brainstem).

Using a parcellation-based *t* test analysis, we identified few regions displaying consistently high normalized [Li] across our cohort despite our modest cohort size and a quite stringent false discovery rate correction [compared with a correction procedure that would account for the correlation between imaging features such as the one proposed by Westfall and Young (49)]. Among those regions were the left middle temporal gyrus, the lateral occipital cortex, and the right pallidum. However, the most well-defined and most significant cluster was the one that corresponded closely with the left hippocampus. To the best of our knowledge, this is the first study reporting such results. This observation is of potential importance for several reasons. First, the hippocampus (along with the amygdala) plays a major role in emotion regulation and processing and in inhibition of stress responses (50). Second, it has been demonstrated that individuals with BD exhibited GM atrophy throughout the entire cortex as well as in subcortical limbic structures (8,51). In particular, the ENIGMA (Enhancing NeuroImaging Genetics through Meta-Analysis) consortium has found that the hippocampus was the subcortical structure with the largest shrinkage in BD (8). The hippocampus thus plays a central role in current neural models of emotion dysregulation in BD (50). Third, other neuroimaging studies have suggested the neuroprotective and neurotrophic effects of Li, which can slow down GM atrophy in BD or may even promote a normalization of GM volumes (50,52), particularly in the hippocampus (9–11,53). Preclinical studies are also supportive of a neurotrophic effect of Li. In particular, Zanni *et al.* (54) have also reported higher concentration levels of Li in the hippocampus of mice using inductively coupled plasma atomic emission spectroscopy, which directly supports our finding. Identifying a consistently high normalized Li concentration specifically in a region could therefore be an intriguing finding and supports the neurogenic hypothesis of Li mode of action. Indeed, the hippocampus seems to be the main location of neurogenesis in the brain (55).

Interestingly, previous neuroimaging studies suggested that the physiopathological processes taking place in the hippocampus of patients with BD could manifest in an asymmetrical way. For instance, both Moorhead *et al.* (56) and Quigley *et al.* (57) have reported smaller left hippocampus volumes among patients with BD compared with healthy control subjects. Also of interest is the observation, in a recent multimodal molecular imaging study (58), of decreased levels of *N*-acetyl-aspartate + *N*-acetyl-aspartyl-glutamate (NAA+NAAG) in the left hippocampus of patients with BD. This decrease was positively correlated with deregulated microglial activation [measured via the ^{11}C-(R)-PK11195 binding potential] and depression symptoms in BD. Furthermore, our observation could be related to asymmetrical effects of Li on hippocampus volume. Indeed, several studies reported larger left hippocampus volume among patients with BD treated with Li compared with patients without Li (59,60). Remarkably, Selek *et al.* (61) highlighted, in a longitudinal volumetric study of patients with BD treated for 4 weeks with Li, a decrease of the left hippocampus volume in Li nonresponders but not in Li responders, suggesting that a decreased left hippocampus volume might be an early marker of nonresponse to Li among patients with BD.

Another interesting result of our study is that [Li] values were highest in the brainstem, midbrain, and cerebellum regions. However, the interindividual variance found for these regions was also very large, as most patients showed elevated concentration levels in those regions while for few others, [Li] in those regions did not exceed the whole-brain average values. Though it is too early to establish a relationship between those observations and the clinical response of Li, it seems relevant to ponder if [Li] in these areas could be linked to some of Li's most problematic side-effects. In particular, chronic toxicity of Li can lead to physiological tremors and ataxia (62), while acute toxicity can lead to permanent loss of eye and speech coordination alongside cerebellar dysfunction (63). Future research is needed to confirm if an elevated [Li] in the brainstem and cerebellar regions could be an indicator that a patient is at risk of neurological Li toxicity.

While those results are promising, especially our ability to identify for the first time, using ^{7}Li MRI, the hippocampus as an area of interest to focus our attention regarding the investigation of Li therapeutic action, it is important to remain humble regarding the limited size of our cohort. As a consequence, we are unable at this stage to account for the potential bias linked to the many sources of interindividual variability, such as sex, age, and the administration of co-medication or eventual addictions, especially alcohol and tobacco.

Finally, this ^{7}Li MRI study represents important scientific and technical steps toward the identification of Li-targeted brain regions involved in Li clinical response in patients with BD. In particular, individual brain [Li] maps hold the promise to inform us about the relationship between the local [Li] and its neuroprotective action as it has been previously evaluated using structural, functional MRI, and ^{1}H magnetic resonance spectroscopy data (64). It also opens avenues to explore to what extent local [Li] correlates with therapeutic response and/or tolerance, as well as the brain regions involved in the different levels of Li response. It would also be of great interest to exploit such data to predict in newly diagnosed patients with BD which ones will benefit from receiving Li.

ACKNOWLEDGMENTS AND DISCLOSURES

The 7T MRI platform received support from the Equipement de Recherche et Plateformes Technologiques program of the Leducq Foundation. This work was funded by the French Ministries of Higher Education, Research, and Innovation and of Social Affairs and Health Inclusion, as well as the French National Research Agency (BIP-Li7 project 2014, Grant No. ANR-14-CE15-0003-01 [to FBe]).

We thank Drs. Sarah Sportiche, Sunthavy Yem, Julia Maruani, and Gregory Gross for their help in recruiting the bipolar patients, as well our colleagues Chantal Ginisty, Severine Roger, Severine Desmidt, Yann Lecomte, Veronique Joly-Testault, Laurence Laurier, Gaëlle Médiouni, Bernadette Martins, and Damien Vanhoye for assisting in the preparation and conduction of the study and Dr. Alexandre Vignaud for his expertise and support.

The authors report no biomedical financial interests or potential conflicts of interest.

ARTICLE INFORMATION

From NeuroSpin (JS, FH, AC, FM, SS, CR-L, JH, ED, FBo), Commissariat à l'Énergie Atomique, Paris-Saclay University, Gif-sur-Yvette; Department of Psychiatry (FH), Corentin-Celton Hospital, Assistance Publique—Hôpitaux de Paris, Issy-les-Moulineaux; Paris University (FH, MM, BE, FBe), Paris; Institut National de la Santé et de la Recherche Médicale U955 Team 15 "Translational Psychiatry" (FH, JH), Paris-East University, Créteil; Siemens Healthineers (FM), Saint-Denis; Saint-Louis–Lariboisière–F. Widal Hospitals (ND-O, JP, MM, BE, FBe), Assistance Publique—Hôpitaux de Paris, Paris; Département Médico-Universitaire de Psychiatrie et d'Addictologie (JH), Mondor University Hospital, Assistance Publique—Hôpitaux de Paris, Créteil; Institut National de la Santé et de la Recherche Médicale UMRS-1144 (MM, BE, FBe), Paris; and FondaMental Foundation (BE, JH, FBe), Créteil, France; and Neurology (SR), Rheinisch-Westfälische Technische Hochschule Aachen University Hospital, Aachen, Germany.

Address correspondence to Fawzi Boumezbeur, Ph.D., NeuroSpin, Centre CEA de Saclay, Bâtiment 145, 91191 Gif-sur-Yvette Cedex, France; E-mail: fawzi.boumezbeur@cea.fr.

Received Sep 19, 2019; revised Jan 14, 2020; accepted Feb 3, 2020.

Supplementary material cited in this article is available online at https://doi.org/10.1016/j.biopsych.2020.02.1181

REFERENCES

1. Merikangas KR, Jin R, He JP, Kessler RC, Lee S, Sampson NA, *et al.* (2011): Prevalence and correlates of bipolar spectrum disorder in the world mental health survey initiative. Arch Gen Psychiatry 68:241–251.
2. Grande I, Berk M, Birmaher B, Vieta E (2016): Bipolar disorder. Lancet 387(10027):1561–1572.
3. Shorter E (2009): The history of lithium therapy. Bipolar Disord 11:4–9.
4. Yatham LN, Kennedy SH, Parikh SV, Schaffer A, Bond DJ, Frey BN, *et al.* (2018): Canadian Network for Mood and Anxiety Treatments (CANMAT) and International Society for Bipolar Disorders (ISBD) 2018 guidelines for the management of patients with bipolar disorder. Bipolar Disord 20:97–170.
5. Bauer MS, Mitchner L (2004): What is a "mood stabilizer"? An evidence-based response. Am J Psychiatry 161:3–18.
6. Baldessarini RJ, Tondo L, Davis P, Pompili M, Goodwin FK, Hennen J (2006): Decreased risk of suicides and attempts during long-term lithium treatment: A meta-analytic review. Bipolar Disord 8(5 pt 2):625–639.
7. Rowe MK, Wiest C, Chuang DM (2007): GSK-3 is a viable potential target for therapeutic intervention in bipolar disorder. Neurosci Biobehav Rev 31:920–931.
8. Hibar DP, Westlye LT, van Erp TG, Rasmussen J, Leonardo CD, Faskowitz J, *et al.* (2016): Subcortical volumetric abnormalities in bipolar disorder. Mol Psychiatry 21:1710.
9. Hallahan B, Newell J, Soares JC, Brambilla P, Strakowski SM, Fleck DE, *et al.* (2011): Structural magnetic resonance imaging in bipolar disorder: An international collaborative mega-analysis of individual adult patient data. Biol Psychiatry 69:326–335.
10. Hajek T, Bauer M, Simhandl C, Rybakowski J, O'Donovan C, Pfennig A (2014): Neuroprotective effect of lithium on hippocampal volumes in bipolar disorder independent of long-term treatment response. Psychol Med 44:507–517.
11. López-Jaramillo C, Vargas C, Díaz-Zuluaga AM, Palacio JD, Castrillón G, Vieta E, *et al.* (2017): Increased hippocampal, thalamus and amygdala volume in long-term lithium-treated bipolar I disorder patients compared with unmedicated patients and healthy subjects. Bipolar Disord 19:41–49.
12. Luo H, Gauthier M, Tan X, Landry C, Cisternino S, Declèves X (2018): Sodium transporters are involved in lithium influx in brain endothelial cells. Mol Pharm 15:2528–2538.
13. Jakobsson E, Argüello-Miranda O, Chiu SW, Fazal Z, Kruczek J, Pritchet L, *et al.* (2017): Toward a unified understanding of lithium action in basic biology and its significance for applied biology. J Membr Biol 250:587–604.
14. Leterrier C, Brachet A, Fache MP, Dargent B (2010): Voltage-gated sodium channel organization in neurons: Protein interactions and trafficking pathways. Neurosci Lett 486:92–100.
15. Wang J, Ou SW, Wang YJ (2017): Distribution and function of voltage-gated sodium channels in the nervous system. Channels (Austin) 11:534–554.
16. Whitaker WR, Clare JJ, Powell AJ, Chen YH, Faull RL, Emson PC (2000): Distribution of voltage-gated sodium channel alpha-subunit and beta-subunit mRNAs in human hippocampal formation, cortex, and cerebellum. J Comp Neurol 422:123–139.
17. Hladky SB, Barrand MA (2016): Fluid and ion transfer across the blood-brain and blood-cerebrospinal fluid barriers; a comparative account of mechanisms and roles. Fluids Barriers CNS 13:19.
18. Severus E, Bauer M, Geddes J (2018): Efficacy and effectiveness of lithium in the long-term treatment of bipolar disorders: An update 2018. Pharmacopsychiatry 51:173–176.
19. Renshaw PF, Wicklund S (1988): In vivo measurement of lithium in humans by nuclear magnetic resonance spectroscopy. Biol Psychiatry 23:465–475.
20. Smith FE, Cousins DA, Thelwall PE, Ferrier IN, Blamire AM (2011): Quantitative lithium magnetic resonance spectroscopy in the normal human brain on a 3 T clinical scanner. Magn Reson Med 66:945–949.
21. Machado-Vieira R, Otaduy MC, Zanetti MV, de Sousa RT, Dias VV, Leite CC, *et al.* (2016): A selective association between central and peripheral lithium levels in remitters in bipolar depression: A 3T-^{7}Li magnetic resonance spectroscopy study. Acta Psychiatr Scand 133:214–220.
22. Komoroski RA, Newton JE, Sprigg JR, Cardwell D, Mohanakrishnan P, Karson CN (1993): In vivo ^{7}Li nuclear magnetic resonance study of lithium pharmacokinetics and chemical shift imaging in psychiatric patients. Psychiatry Res 50:67–76.
23. Ramaprasad S, Ripp E, Pi J, Lyon M (2005): Pharmacokinetics of lithium in rat brain regions by spectroscopic imaging. Magn Reson Imaging 23:859–863.
24. Lee JH, Adler C, Norris M, Chu WJ, Strakowski SM, Komoroski RA (2012): 4-T ^{7}Li 3D MR spectroscopy imaging in the brains of bipolar disorder subjects. Magn Reson Med 68:363–368.
25. Gyulai L, Wicklund SW, Greenstein R, Bauer MS, Ciccione P, Whybrow PC, *et al.* (1991): Measurement of tissue lithium concentration by lithium magnetic resonance spectroscopy in patients with bipolar disorder. Biol Psychiatry 29:1161–1170.
26. Ramaprasad S, Newton JEO, Cardwell D, Fowler AH, Komoroski RA (1992): In vivo ^{7}Li NMR imaging and localized spectroscopy of rat brain. Magn Reson Med 25:308–318.
27. Komoroski RA, Pearce JM, Newton JE (1997): The distribution of lithium in rat brain and muscle in vivo by ^{7}Li NMR imaging. Magn Reson Med 38:275–278.
28. Smith FE, Thelwall PE, Necus J, Flowers CJ, Blamire AM, Cousins DA (2018): 3D ^{7}Li magnetic resonance imaging of brain lithium distribution in bipolar disorder. Mol Psychiatry 23:2184.
29. Stout J, Hanak AS, Chevillard L, Djemaï B, Bellivier F, Boumezbeur F, *et al.* (2017): Investigation of lithium distribution in the rat brain ex vivo using lithium-7 magnetic resonance spectroscopy and imaging at 17.2 T. NMR Biomed 30:e3770.
30. Boada FE, Gillen JS, Shen GX, Chang SY, Thulborn KR (1997): Fast three dimensional sodium imaging. Magn Reson Med 37:706–715.
31. Qian Y, Boada FE; University of Pittsburgh (2010): Method for producing a magnetic resonance image of an object having a short T2 relaxation time. U.S. patent 7,750,632. Patent granted July 6, 2010.
32. Montgomery SA, Åsberg M (1979): A new depression scale designed to be sensitive to change. Br J Psychiatry 134:382–389.
33. Young RC, Biggs JT, Ziegler VE, Meyer DA (1978): A rating scale for mania: Reliability, validity and sensitivity. Br J Psychiatry 133:429–435.
34. Nurnberger JI, Blehar MC, Kaufmann CA, York-Cooler C, Simpson SG, Reich T, *et al.* (1994): Diagnostic interview for genetic studies: Rationale, unique features, and training. Arch Gen Psychiatry 51:849–859.
35. Hanak AS, Chevillard L, El Balkhi S, Risede P, Peoc'h K, Megarbane B (2014): Study of blood and brain lithium pharmacokinetics in the rat

according to three different modalities of poisoning. Toxicol Sci 143:185–195.
36. Manchia M, Adli M, Akula N, Ardau R, Aubry JM, Alda M, *et al.* (2013): Assessment of response to lithium maintenance treatment in bipolar disorder: A Consortium on Lithium Genetics (ConLiGen) report. PLoS One 8:e65636.
37. Freeman R, Hill HDW (1971): Fourier transform study of NMR spin–lattice relaxation by "progressive saturation. J Chem Phys 54:3367–3377.
38. Jackson JI, Meyer CH, Nishimura DG, Macovski A (1991): Selection of a convolution function for Fourier inversion using gridding (computerised tomography application). IEEE Trans Med Imaging 10:473–478.
39. Noll DC, Pauly JM, Meyer CH, Nishimura DG, Macovskj A (1992): Deblurring for non-2D Fourier transform magnetic resonance imaging. Magn Reson Med 25:319–333.
40. Man LC, Pauly JM, Macovski A (1997): Multifrequency interpolation for fast off-resonance correction. Magn Reson Med 37:785–792.
41. Nylund A (2014): Off-resonance correction for magnetic resonance imaging with spiral trajectories [dissertation]. Available at: http://urn.kb.se/resolve?urn=urn:nbn:se:kth:diva-147925.
42. Wellcome Centre for Human Neuroimaging. Statistical parametric mapping. Available at: http://www.fil.ion.ucl.ac.uk/spm/.
43. Bernstein MA, King KF, Zhou XJ (2004): Handbook of MRI Pulse Sequences. Elsevier.
44. University of Oxford. Templates and atlases included with FSL. Available at: https://fsl.fmrib.ox.ac.uk/fsl/fslwiki/Atlases.
45. Makris N, Goldstein JM, Kennedy D, Hodge SM, Tsuang MT, Seidman LJ, *et al.* (2006): Decreased volume of left and total anterior insular lobule in schizophrenia. Schizophr Res 83:155–171.
46. Frazier JA, Chiu S, Breeze JL, Makris N, Caviness VS, Biederman J, *et al.* (2005): Structural brain magnetic resonance imaging of limbic and thalamic volumes in pediatric bipolar disorder. Am J Psychiatry 162:1256–1265.
47. Benjamini Y, Hochberg Y (1995): Controlling the false discovery rate: A practical and powerful approach to multiple testing. J R Stat Soc Ser B 57:289–300.
48. Komoroski RA, Lindquist DM, Pearce JM (2013): Lithium compartmentation in brain by ^{7}Li MRS: Effect of total lithium concentration. NMR Biomed 26:1152–1157.
49. Westfall PH, Young SS, Paul Wright S (1993): On adjusting *p* values for multiplicity. Biometrics 49:941–945.
50. Phillips ML, Swartz HA (2014): A critical appraisal of neuroimaging studies of bipolar disorder: Toward a new conceptualization of underlying neural circuitry and a road map for future research. Am J Psychiatry 171:829–843.
51. Hibar DP, Westlye LT, Doan NT, Jahanshad N, Cheung JW, Krämer B, *et al.* (2018): Cortical abnormalities in bipolar disorder: An MRI analysis of 6503 individuals from the ENIGMA Bipolar Disorder Working Group. Mol Psychiatry 23:932–942.
52. Moore GJ, Bebchuk JM, Wilds IB, Chen G, Menji HK (2000): Lithium-induced increase in human brain grey matter. Lancet 356(9237):1241–1242.
53. Foland LC, Altshuler LL, Sugar CA, Lee AD, Leow AD, Thompson PM, *et al.* (2008): Increased volume of the amygdala and hippocampus in bipolar patients treated with lithium. Neuroreport 19:221–224.
54. Zanni G, Michno W, di Martino E, Tjärnlund-Wolf A, Blomgren K, Hanrieder J, *et al.* (2017): Lithium accumulates in neurogenic brain regions as revealed by high resolution ion imaging. Sci Rep 7:40726.
55. Moreno-Jiménez EP, Flor-García M, Cafini F, Pallas-Bazarra N, Ávila J, Llorens-Martín M, *et al.* (2019): Adult hippocampal neurogenesis is abundant in neurologically healthy subjects and drops sharply in patients with Alzheimer's disease. Nat Med 25:554–560.
56. Moorhead TW, McKirdy J, Sussmann JE, Hall J, Lawrie SM, Johnstone EC, McIntosh AM (2007): Progressive gray matter loss in patients with bipolar disorder. Biol Psychiatry 62:894–900.
57. Quigley SJ, Scanlon C, Kilmartin L, Barker GJ, Cannon DM, McDonald C, *et al.* (2015): Volume and shape analysis of subcortical brain structures and ventricles in euthymic bipolar I disorder. Psychiatry Res 233:324–330.
58. Haarman B, Burger H, Doorduin J, Renken RJ, Mendes R, Nolen WA, *et al.* (2016): Volume, metabolites and neuroinflammation of the hippocampus in bipolar disorder—A combined magnetic resonance imaging and positron emission tomography study. Brain Behav Immun 56:21–33.
59. Zung S, Souza-Duran FL, Soeiro-de-Souza MG, Uchida R, Busatto GF, Vallada H, *et al.* (2016): The influence of lithium on hippocampal volume in elderly bipolar patients: A study using voxel-based morphometry. Transl Psychiatry 6:e846.
60. Hajek T, Cullis J, Bauer M, Young LT, Macqueen G, Alda M, *et al.* (2012): Hippocampal volumes in bipolar disorders: Opposing effects of illness burden and lithium treatment. Bipolar Disord 14:261–270.
61. Selek S, Nicoletti M, Zunta-Soares GB, Matsuo K, Sanches M, Soares JC, *et al.* (2013): A longitudinal study of fronto-limbic brain structures in patients with bipolar I disorder during lithium treatment. J Affect Disord 150:629–633.
62. Sadosty AT, Groleau GA, Atcherson MM (1999): The use of lithium levels in the emergency department. J Emerg Med 17:887–891.
63. Niethammer M, Ford B (2007): Permanent lithium-induced cerebellar toxicity: Three cases and review of literature. Mov Disord 22:570–573.
64. Machado-Vieira R (2018): Lithium, stress, and resilience in bipolar disorder: Deciphering this key homeostatic synaptic plasticity regulator. J Affect Disord 233:92–99.